Open Access Journal

Journal of Sustainable Research in Engineering Vol. 8 (1) 2024, 17-24

Journal homepage: https://jsre.jkuat.ac.ke

ISSN (Online): 2409-1243

Identification of grinding kinetics of malachite copper ore using population balance model

Mathew N. Kyalo[1*], James. K. Kuria[1], Hiram. N. Ndiritu[1], Dadson M. Thuku[3]

[1]*Department of Mechanical Engineering, Jomo Kenyatta University of Agriculture and Technology, P. O. Box 62000-00200, Nairobi*

[2]*Engineering Department, Match Electricals Limited. P.O. Box 6086-01000, Thika*

[*]*Corresponding Author - E-mail: mnkyalo@jkuat.ac.ke*

Abstract To liberate copper from malachite, the ore has to be reduced to appropriate size using comminution processes. Ball mills are commonly used to obtain fine particles in grinding circuits. Population balance equations can be used to model grinding kinetics in a ball mill. The aim of this study was to understand the mineralogical characteristics of malachite copper ore and identify its grinding kinetics. To achieve this, chemical analysis and petrographic studies on thin slides were carried out. Additionally, grinding tests were carried out in a ball mill using five mono-sized fractions. Short grinding cycles of 0.5 minutes were used to calculate breakage distribution functions. Longer grinding cycles up to 30 mis were used to determine specific breakage rates. The experimental results were fitted into population balance models to obtain breakage parameters that characterize the material. The parameters were used to predict particle distributions. The malachite bearing copper was found to exists among other minerals. The average concentration of copper was found to be 4.7%. The specific rate of breakage increased as particle size increased to a maximum value at particle size of 2 mm. The parameters of grinding kinetics computed parameters were applied in prediction of particle size distribution. The particle distribution produced a high degree of agreement between the simulated and experimental results. The parameters can be used in the design of ore flowsheets for processing malachite ore.

Keywords: Malachite, ball mill, population balance, grinding kinetics.

1. Introduction

Copper metal is used in vast areas of industry and technology due to special properties, such as high thermal and electrical conductivity, high ductility, and corrosion resistance [1]. Society's plans for a decarbonized world will rely on renewable energy and transport electrification, which are copper-intensive sectors [2]. Copper annual demand is projected to reach 36.6 million tons by 2031, compared to the current demand of about 25 million tons [3]. To meet the increasing demand of copper, efforts to explore and extract various copper ores need to be extended. Copper mining activities will struggle to meet this growing demand as discovery rates of new copper deposits are lagging, and current operating mines are declining [4]. Copper is extracted from various minerals such as chalcopyrite bornite chalcocite, , cuprite, malachite, and azurite [2]. The copper bearing minerals can be further classified into oxides or sulfides. The primary mineral chalcopyrite contains copper up to 34% by weight [5]. The existing deposits of primary copper sulfide ore have continued to decline over the years. The increasing demand of copper will require alternative ore sources like malachite.

Copper ore occurs at various locations in Kenya. In Macalder and Kitere located in western region, sulfide copper deposits with grades in the rage of 3-4.6 percent have been identified [6]. Occurrence of copper has been

reported in Voi hills and Maungu with mineralization up to 8.2 percent [7]. Other studies in Tharaka Nithi have reported chalcoprite assaying in the range of 1.8-8.4% [7]. Malachite copper in the rage of 3-8% has been identified in Kanzugo area in Kitui area within ingenious rocks [8]. In Kazungo area, the mineralization of malachite ore occurs at disseminated localities striking from southwest to northeast [6]. Another area in close proximity to Kanzungo is Mithikwani in Matinyani with similar mineralization.

Malachite [Cu2CO3(OH)2] is formed by weathering of primary copper minerals such as chalcopyrite and bornite copper deposits [9]. It can be identified by its distinct green color, monoclinic crystal system with perfect cleavage and penetration twinning [10]. Petrographic studies are used in identification of malachite. Malachite like other minerals behave differently under different light conditions making it diminish under one light condition say PPL (plane-polarized light) and visible under another say XPL (crossed polarized light). Having both XPL and PPL images, therefore, maximizes the chances of identification of mineral crystals forming a rock sample. Processing of malachite ore starts by comminution, involving crushing and grinding to increase the surface area of the ore for further processing. After comminution, malachite ore is usually processed through a hydrometallurgical method consisting of leaching, solvent extraction and electrolysis [11]. Particle size and distribution is one of most important parameters that affects the leaching of copper. Leaching copper from malachite ore has been studied widely considering choice of media, particle size, and environment conditions [12]–[16]. The rate of leaching of malachite ore has been found to be inversely proportional to the particle size. To reduce particles size, a process comminution circuit is designed for a particular ore. The processes of comminution consume about 50% the of mine site energy [17]. Therefore, it requires optimization to avoid energy wastage or to avoid producing more fine particles that are not suitable for downstream processes [18]. Grinding using a ball mill is one of the final stages of particle reduction in comminution.

In ball milling, a population balance model is used to predict the particle size distribution of the milled material as a function of the material properties, and milling conditions. The approach entails determination of selection and breakage functions to describe the grinding kinetics. Researchers have used this approach in the past considering breakage of course particles and energy efficiency [19]–[21]. The outcome of the efforts has led to better understanding improvement of grinding processes for a variety of ores. It is evident in literature that research on grinding of copper ore has been focused on copper sulfides ores [14],[19]. The aim of this study was to analyze the mineralogical characteristics and evaluate the grinding kinetics of malachite ore. The grinding kinetics data will be used in development of a pilot plant comprising of all the processes of liberation of copper from malachite ore. The main focus was the selection of feed size and prediction of particle distribution. Parameters values obtained from kinetic model-based grinding are suitable for simulation of large-scale processing of ore. The understanding of the milling kinetics of malachite copper ore will contribute in development of grinding circuits.

2. Theory

In ball milling, a first order population balance equation is used to model probability of breakage of particles of a certain size into smaller class sizes. The equation is based two main functions namely; specific rate of breakage, S_i and breakage function, b_{ij} [23], [24]. The specific rate of breakage S_i (also known as probability of breakage) denotes the top size class of particles that will be broken during milling i.e., the specific breakage rate of particles in class of size 'i'. The breakage function (also called distribution function) b_{ij} denotes the distribution of progenies after breakage in size class 'j'. The model assumes that the mill is fully mixed i.e. no segregation of material into sizes inside the mill. Using the two functions, it is possible to express the size-mass balance equation for a particle class using equation (1),

$$\frac{dm_i(t)}{dt} = -S_i m_i(t) + \sum_{\substack{j=1 \\ i<j}}^{i-1} b_{i,j} S_j \, m_j(t) \qquad (1)$$

where $m_i(t)$ is the mass fraction of the particles of component i, S_i is the specific rate of breakage, $b_{i,j}$ is the rate at which particles of the ground component i, become particles of component j, and t is the grinding time. When $i = 1$, equation (1) can be simplified to take the form equation (2) [25],

$$\frac{dm_i(t)}{dt} = -S_1 m_1(t) \qquad (2)$$

where S_1 is a specific rate of breakage of size 1 material and $m_1(t)$ is the fraction by weight of the material of size 1 at time t. If S_1 is constant with time, then equation (2) can be written in the form of equation (3). The value of S_1 can be determined from the slope of $[m_1(t)]/m_1(0)$ versus time on a semi-log plot [26].

$$Log[m_1(t)] = Log[m_1(0)] - \frac{S_1.t}{2.303} \quad (3)$$

Equation (3) is termed as the first-order kinetics of grinding.

Particle breakage of a single feed size fraction in a ball mill usually fits first order kinetics. Nevertheless, buildup of fines that cushion particle breakage and inappropriate milling conditions might lead to second order breakage [26]. Second order breakage can be modeled using Barani et.al second order breakage equation [27]. To maintain first order breakage, short grinding cycles are selected for experiments, to minimize accumulation of fines that can cushion particle breakage resulting to deviation from first order kinetics. Additionally, the grinding conditions are selected such that the available energy of the grinding media is sufficient to break the particles.

According to L. G. Austin [23], the specific rate of breakage for a particular class size can be fitted using equation (4),

$$S_i = \frac{\mathrm{a}x_i^{\alpha}}{1 + \left(\frac{x_i}{\mu}\right)^{\Lambda}} \quad (4)$$

where a and μ are model parameters related to the grinding conditions, x_i is the particle size in class i in mm, and α and Λ are material properties. These parameters are obtained from a log-log graph of specific breakage versus particle size. When material of size j breaks once, the mass fraction of the broken products with size i can be represented by the breakage function $b_{i,j}, i > j$ [28]. The breakage function is usually represented in cumulative form $b_{i,j}$ as shown in equation (5),

$$B_{i,j} = \sum_{k=n}^{i} b_{k,j} \quad (5)$$

where $b_{k,j} = b_{i,j} - b_{i+1,j}$

If the grinding cycles are short, producing 20-30 percent breakage of the top size, $B_{i,j}$ can be estimated from analysis of milling product size using a narrow size j fraction as initial feed as shown in equation (6). This method is one the one-size fraction BII method shown in equation [29],

$$B_{i,j} = \frac{log[(1 - P_i(0))/(1 - P_i(t))]}{\log[(1 - p_{j+1}(0))/(1 - p_{j+1}(t))]} \quad (6)$$

where $p_i(t)$ is the mass fraction less than x_i size at time t. Another method of representing the cumulative particle breakage, $B_{i,j}$ is by using the following empirical form shown in equation (7) suggested by L.G. Austin [29],

$$B_{i,j} = \Phi_j \left(\frac{x_{i-1}}{x_j}\right)^{\gamma} + (1 - \Phi_j).\left(\frac{x_{i-1}}{x_j}\right)^{\beta}, i > j \quad (7)$$

where x_j is the top size, Φ_j, γ and β are model parameters that depend on the properties of the materials.

3. Methodology

The material used in the present experimental study was copper ore obtained from Muthikwani in Matinyani division, Kitui West Constituency in Kenya (1.3551° S, 37.7194° E). The copper ore was obtained from an area approximately 200 m x 4 m and a depth of 2.5m. The size of the sample was sufficient to stockpile for a pilot plant in construction at Match electricals located in Thika town. The overburden was stripped to a depth of one meter and the bare rock was drilled and blasted. The blasting agent used was ammonium nitrate/fuel oil (ANFO). The run of mines (ROM) ore was hauled by trucks and stockpiled in Match electricals yard. Four rock samples were picked at random and polished into thin sections at the Mining, Blue Economy and Maritime affairs labs in Nairobi for petrographic analysis and chemical composition analysis. The chemical composition was done using X-ray Fluorescence Spectroscopy (XRF) and analyzed using Bruker Esprit 1.9 software. The ore from stockpiles was crushed using a jaw crusher (PE 250X400 mm) at Match electricals into particles with an upper class of 40 mm. The crushed particles were obtained from the crusher at intervals of 20 minutes. The sampled material was thoroughly mixed to obtain 200 kgs. The sample was further crushed using a laboratory jaw crusher at JKUAT Engineering workshops and classified to obtain samples in the following standard size classes; –3.35+2.36 mm, –2.36+2.00 mm, –2.00 +1.70 mm, –1.70+1.40 mm, -1.40+1.00 mm. The range of particle sizes are within ASTM 11 sieve designation. Each sample was split into four batches using cone and quartering method for grinding experiments. The volume occupied by grinding media J, and material filling f_c, were calculated

according to E. Petrakis et.al [28], using equation (8) and equation (9) respectively,

$$J = \left(\frac{V_b}{V_m}\right).\frac{1}{1-\varepsilon} \quad (8)$$

$$f_c = \left(\frac{V_p}{V_m}\right).\frac{1}{1-\varepsilon} \quad (9$$

where V_b is the volume of solid grinding media, V_p the volume of solid powder, V_m is mill volume and ε is the bed porosity of grinding media assumed to be 0.4. Interstitial filling U was calculated using equation (10).

$$U = \frac{f_c}{\varepsilon.J} \quad (10)$$

The milling kinetics tests were carried out in a ball mill with internal diameter of 0.362 m and length of 0.540 m, whereas the effective volume total capacity is 52.7 liters. Industrial mills operate at grinding media bed of 30-45% and interstitial filling of 100%. The conditions used are based on optimal laboratory conditions developed in the laboratory. These conditions are listed in Table 1. The milling tests were run at different grinding intervals, t (0.5, 1, 2, 5, 10, 15, and 30 min). Then particle size distributions were characterized using a series of screens with a ratio of $\sqrt{2}$ for the determination of particle size distribution. Primary breakage distribution function, was determined using L. Austin's BII method for short grinding cycles of 0.5 min for each size fraction [30]. The mill was stopped after each time interval to remove a sample of 200 grams. The material retained on the screens, was returned to the mill to continue to the subsequent griding time.

Table 1. Laboratory ball mill operating conditions

Mill	Diameter 0.362 m Critical speed (C); 70.8rpm Operating speed; 49.6 (0.7C)
Filling	Grinding media bed, J; 30% Ore interstitial filling, U; 67% Ore volume fraction, fc; 0.08
Grinding media	Material: Alloy steel Specific density 7.75 g/cm3 Distribution 38 mm (30%), 25 mm (60%), & 19 mm (30%) Bulk density 4460 kg/m3,

The specific breakage rates (S_i) were determined by plotting the fraction retained on the top size for each size interval against time according to equation (3). The obtained values were fitted equation (4) to obtain the model parameters *a, α, μ,* and *Λ*. Equation (6) was used to calculate breakage function for each feed size. An online calculator that uses all the differential equations of a population balance model used to calculate breakage parameters β, γ, and ∅ [31]. Equation (11) is used to obtain optimal combination of parameters that minimizes the residual error between the experimental and predicted size distributions.

$$\varphi = \sum_{i=1}^{n} w_i \left(\frac{F_i - R_i}{R_i}\right)^2 .100\% \quad (11)$$

where F_i represents the particle size distribution of the mill product (as % retained on screen xi), R_i represents the response of each corresponding F_i for a given set of model parameters, n is the number of screen intervals used and w_i is the average weight factor for each screen that quantifies the relative quality and reliability of each particular screen size value with respect to the other values (high values indicate more reliable measurements). At least four size distributions acquired at four grinding periods are required for the program.

4. Results and Discussion

4.1. Ore mineralogy

The hand specimens of the ore were massive, light green in color with a dull lustre, and a phaneritic texture. A sample results of petrographic studies is shown in Figure 1. The specimen shows presence of biotite that appeared stained with a secondary mineral preferably malachite, it appears altered. The groundmass consists quartz, feldspar, biotite among other minerals. Malachite is the copper bearing mineral characterized by green colour. Chemical compositions obtained using X-ray Fluorescence Spectroscopy (XRF) and analyzed using Bruker Esprit 1.9 software is shown in Table 2.

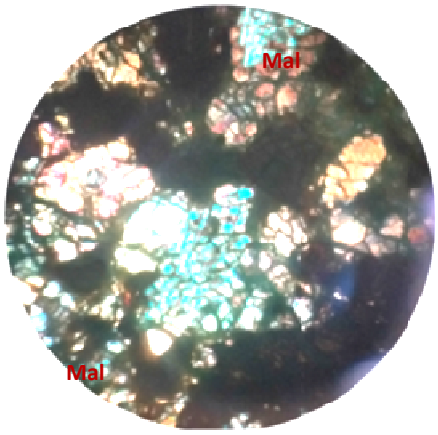

Figure 1: Photomicrograph of crossed polarized light (XPL) of malachite bearing ore showing minerals such as malachite (Mal), biotite (Bt), quartz (Qtz),) and feldspar (Fds).

Table 2: chemical composition of feed material (wt. %).

MgO	Al_2O_3	SiO_2	CaO	Fe	Cu
7.84	15.20	52.37	9.43	7.57	4.76

The results represent average values of three samples obtained randomly during crushing. The percentage composition of copper 4.76% confirms the presence of copper in the ore. The ore bearing mineral is classified as malachite from physical observation, petrographic studies and chemical composition analysis. The area of study is within the Mozambique belt mainly covered by rocks of the basement system [32]. In the area malachite ore is assayed in the range 3-8 percent of copper, similar range as the obtained result for Mithikwani area.

4.2. Specific rate of breakage

To obtain specific rate of breakage (S_i), the percentage mass retained on the top screen was plotted against the grinding time (t) on a log-linear scale for all feed sizes. The value S_i was calculated from the gradient graph of % mass fraction retained versus time shown in Figure 2. Each test was carried out in duplicate and the error in the results was generally less than 2%. An average value was recorded to improve reliability of the results. Table 3 shows calculated values of $S_i$values for each mono-size. It can be observed that finer particles are difficult to break, this can be attributed to reduced nipping capabilities of fine particles in the mill. Both the number and size of defects inherent in minerals decrease with decreasing particle size [33]. Reduced size and number of defects require higher forces to break the finer particle. As particle size increased, the magnitudes of the specific rate of breakage also increased, but dropped after the particle size reached 2 mm. As the particle size increased beyond 2 mm under constant milling conditions, the energy from grinding media was not sufficient to effectively break larger particles. This value was taken as the optimum feed size under the operating conditions. Beyond this size, the ore sample is too large and strong to broken by the grinding media present [34]. The specific rates of breakage (S_i) consequently dropped. The calculated S_i values for each mono feed size were fitted in Eq. (4) using non-linear regression technique to estimate the equation parameters. The calculated values are shown in Table 4. The parameter Λ governs how fast the specific rate of breakage, decreases as the feed size increase. The fine mono-sizes had the highest rate of decrease in specific rate of breakage.

Table 3: specific breakage function values for all feed size classes

Classes mono-sized malachite materials (mm)	Selection function values (Si)
–3.350+2.360	1.345
–2.360+2.000	2.441
–2.000+1.700	2.892
–1.700+1.400	0.534
–1.400+1.000	0.055

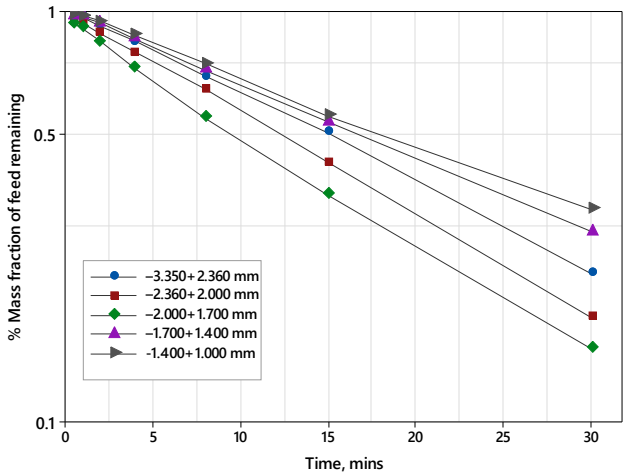

Figure 2: First order grinding plots for Malachite ore

Table 4: specific breakage function parameters

Classes mono-sized malachite materials (mm)	a	α	μ	Λ
–3.350+2.360	1.00	0.62	3.47	1.73
–2.360+2.000	1.02	0.70	4.71	1.57
–2.000+1.700	1.56	0.87	5.01	2.00
–1.700+1.400	0.41	2.36	4.97	2.30
–1.400+1.000	0.51	2.34	4.63	2.30

4.3. Breakage distribution

Primary breakage function parameters were calculated using equation (6), for the shortest grinding cycle of 0.5 minutes. The cumulative breakage distribution functions of the malachite ore at different initial feed sizes are shown in Figure 3. The graph shows typical normalized behavior so that the output particles distribution was independent of the feed particle size. The parameters of breakage function γ, β, and ∅ were estimated using equation (7) and are listed in Table 5. The values of ∅ is for all mono-sized samples were close with a standard deviation of 0.0083 indicating a similar breakage of the top size. The parameters γ and β are postulated to represent breakage mechanism of cleavage and shattering respectively [35]. In crystals, cleavage is defined as the breakage along the preferred material surfaces; in contrast, shattering happens when the loading is perpendicular to the particle and the supplied energy is greater than what is needed for cleavage breakage. [36]. Based on the mechanisms of breakage, it can be concluded that the breakage mechanism of the material was both cleavage and shattering. Further, it has been postulated that higher value γ indicate lower reduction ratios [37]. The finer sizes had higher values indicating lower reduction ratios. The average breakage function values obtained are close to those obtained in Etoile mine copper-cobalt for a copper ore in a pear shaped ball mill pilot test [28].

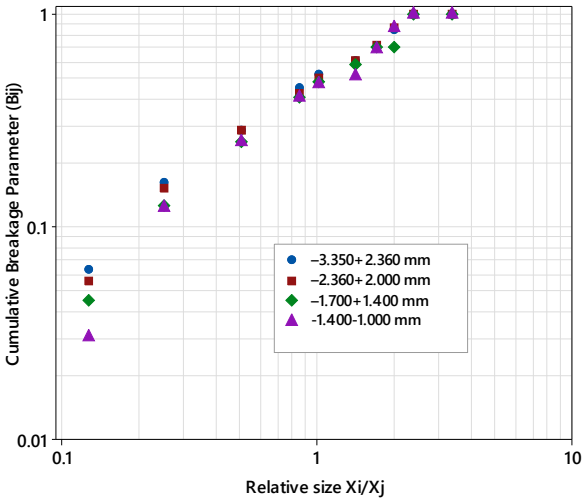

Figure 3: Cumulative breakage function distributions for different initial feed sizes of malachite ore

Table 5: Primary breakage distributions parameters for various feed sizes

Classes mono-sized malachite materials (mm)	γ	β	$\emptyset$
–4.750+3.350	0.85	5.5	0.81
–3.350+2.360	0.85	5.3	0.81
–2.360+2.000	0.86	5.18	0.82
–2.000+1.700	0.96	5.11	0.82
–1.700+1.400	0.98	5.49	0.83
Average	0.9	5.13	0.82

The calculated specific breakage parameters (α, Λ, γ and μ) and breakage distribution parameters (β, γ, and ∅) were used to reproduce size distribution of the grinding products using online calculator. During simulation, breakage distribution values were considered to be independent of the initial size i.e dimensionally normalizable. To reduce the residual error between the experimental and predicted product size distributions, the model searches for the optimal combination of these parameters.

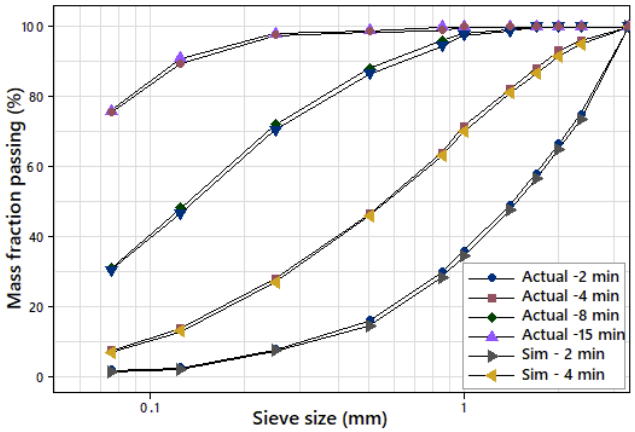

Figure 4: Predicted and measured particle size distributions of the malachite ore

Figure 4 shows the measured and predicted size distributions for all milling products. It can be observed that the simulated size distributions, in the plotted graphs coincide fairly well with average error in the range of 1.98-2.3%. This enabled the kinetics model to be verified and provided evidence that the selection and breakage functions parameters can be applied to a continuous mass balance.

5. Conclusion

Chemical composition of the ore revealed an average copper element composition of 4.76%. The copper bearing mineral was malachite existing with other minerals like quartz, biotite and feldspar. The kinetics of the malachite ore milling was studied using population balance model. The selected mono-sized fractions show typical normalized behavior as the progeny particle distributions were independent of the feed particle size. An optimum particle size upper of 2.00mm was determined under the present milling conditions. The average breakage function values for malachite ore from Mithikwani were: $\beta = 5.13$, $\gamma = 0.9$ and $\Phi = 0.82$. The mechanism of breakage was attributed to both cleavage and shattering. The breakage behavior at laboratory scale may not accurately reflect the industrial scale milling but can give good insights on how malachite ore will perform in milling circuits. This finding will be used in development of a pilot plant for processing of malachite ore. The results can also be used in setting up grinding circuit models for industrial malachite ore flowsheets. In future the effect of ball size and distribution and interstitial fill on milling of malachite can be studied. Further, geological studies should be conducted in future to map the ore body and evaluate economics of mining.

Acknowledgement

The authors are grateful to African Development Bank (AfDB), through the Ministry of Education, Science & Technology for funding the research. We also acknowledge the management of Match Electrical Limited for provision and preparation of malachite copper ore sample that was used in this study.

Abbreviations and Symbols

ANFO	*ammonium nitrate/fuel oil*
a	*model parameters related to the grinding conditions*
$b_{i,j}$	*breakage distribution*
C	*ball mill critical speed*
d	*ball diameter (mm)*
f_c	*material filling*
F_i	*particle size distribution of the mill product (as % retained on screen*
J	*grinding media bed, (%)*
L	*mill length, (m)*
$m_i(t)$	*mass fraction of particles*
n	*number of screen intervals*
PPL	*plane-polarized light*
R_i	*response of each corresponding particle size distribution for a given set of model parameters,*
ROM	*run of mines*
S_i	*specific rate of breakage*
t	*time*
U	*interstitial filling*
V_b	*is the volume of solid balls,*
V_m	*is mill volume and*
V_p	*the volume of solid powder,*
w_i	*average weight factor for each screen*
x_i	*Particle size in class i in mm,*
XPL	*crossed polarized light*
XRF	*X-ray Fluorescence Spectroscopy*
α	*model parameters normally in the range 0.5 to 1.5*
β	*model parameters that depend on the properties of the material*
γ	*model parameters that depend on the properties of the material*
ε	*bed porosity of grinding media*
Λ	*index of how rapidly the rates of breakage fall as size increases*
μ	*optimum particle size for particular mill conditions*
Φ_j	*model parameters that depend on the*

properties of the material

References

[1] International Copper Study Group, "The World Copper Factbook 2016," *Int. Copp. Study Gr.*, p. 63, 2016.

[2] D. A. Singer, "Future copper resources," *Ore Geol. Rev.*, vol. 86, pp. 271–279, Jun. 2017.

[3] S. van Z. Scott Crooks, Jonathan Lindley, Dawid Lipus, Richard Sellschop, Eugéne Smit, "Metals & Mining Practice - Bridging the copper supply gap," 2023.

[4] M. Noaparast, S. Rahmati, G. Jozanikohan, S. Aslani, and A. Ghorbani, "A Methodology to Estimate Ores Work Index Values, Using Miduk Copper Mine Sample," *Int. J. Min Geo-Eng*, vol. 46, no. 2, pp. 133–140, 2012.

[5] S. S. Jena, S. K. Tripathy, N. R. Mandre, R. Venugopal, and S. Farrokhpay, "Sustainable Use of Copper Resources: Beneficiation of Low-Grade Copper Ores," *Minerals*, vol. 12, no. 5, 2022.

[6] L. D. Sanders, "Geology of the Kitui Area," Nairobi, 2007.

[7] E. P. Saggerson, "Geology of the Kasigau-Kurase area," 1958.

[8] P. M. Kugeria, "Extraction of copper using chicken dung and concentration of titanium using biomass from ores in Maragwa location, Tharaka Nithi county," The University of Embu, 2020.

[9] S. K. Haldar, "Introduction," in *Platinum-Nickel-Chromium Deposits*, Elsevier, 2017, pp. 1–35.

[10] S. K. Haldar, "Minerals and rocks," in *Introduction to Mineralogy and Petrology*, 2020, pp. 1–51.

[11] M. B. Hocking, "Ore Enrichment and Smelting of Copper," *Handb. Chem. Technol. Pollut. Control*, pp. 391–420, 2005.

[12] B. C. Tanda, E. A. Oraby, and J. J. Eksteen, "Kinetics of malachite leaching in alkaline glycine solutions," *Miner. Process. Extr. Metall. Trans. Inst. Min. Metall.*, vol. 130, no. 1, pp. 16–24, 2021.

[13] M. A. Shabani, M. Irannajad, and A. R. Azadmehr, "Investigation on leaching of malachite by citric acid," *Int. J. Miner. Metall. Mater.*, vol. 19, no. 9, pp. 782–786, 2012.

[14] M. J. Nicol, "The kinetics of the dissolution of malachite in acid solutions," *Hydrometallurgy*, vol. 177, pp. 214–217, 2018.

[15] S. Y. Seoa, W. S. Choia, M. J. Kima, and T. Trana, "Leaching of a Cu-Co ore from Congo using sulphuric acidhydrogen peroxide leachants," *J. Min. Metall. Sect. B Metall.*, vol. 49, no. 1, pp. 1–7, 2013.

[16] O. N. Ata, S. Çolak, Z. Ekinci, and M. Çopur, "Determination of the optimum conditions for leaching of malachite ore in H2SO4 solutions," *Chem. Eng. Technol.*, vol. 24, no. 4, pp. 409–413, 2001.

[17] J. Jeswiet and A. Szekeres, "Energy Consumption in Mining Comminution," *Procedia CIRP*, vol. 48, pp. 140–145, 2016.

[18] A. Ebadnejad, "Investigating of the effect of ore work index and particle size on the grinding modeling of some copper sulphide ores," *J. Mater. Res. Technol.*, vol. 5, no. 2, pp. 101–110, Apr. 2016.

[19] R. R. Klimpel and L. G. Austin, "The back-calculation of specific rates of breakage and non-normalized breakage distribution parameters from batch grinding data," *Int. J. Miner. Process.*, vol. 4, no. 1, pp. 7–32, 1977.

[20] M. Capece, E. Bilgili, and R. Dave, "Identification of the breakage rate and distribution parameters in a non-linear population balance model for batch milling," *Powder Technol.*, vol. 208, no. 1, pp. 195–204, 2011.

[21] V. K. Gupta, "Determination of the specific breakage rate parameters using the top-size-fraction method: Preparation of the feed charge and design of experiments," *Adv. Powder Technol.*, vol. 27, no. 4, pp. 1710–1718, 2016.

[22] C. Mudenda, B. G. Mwanza, and M. Kondwani, "Analysis of the Effects of Grind Size on Production of Copper Concentrate : A Case Study of Mining Company in Zambia," *Int. J. Sci. Basic Appl. Res.*, pp. 259–268, 2015.

[23] L. G. Austin, K. Shoji, and P. T. Luckie, "The effect of Ball Size on Mill Perfomance," *Powder Technol.*, vol. 14(1976), pp. 71–79, 1975.

[24] V. Sogani, P. Somani, N. Singla, and R. Mathur, "POPULATION BALANCE IN BALL MILL," *Int. J. Innov. Res. Technol.*, vol. 3, no. 2, pp. 2349–6002, 2016.

[25] L. G. Austin, "A commentary on the Kick, Bond and Rittinger laws of grinding," *Powder Technol.*, vol. 7, no. 6, pp. 315–317, Jun. 1973.

[26] M. . Celik, "Acceleration of breakage rates of anthracite during grinding in a ball mill," *Powder Technol.*, vol. 54, no. 4, pp. 227–233, Apr. 1988.

[27] K. Barani and H. Balochi, "First-order and second-order breakage rate of coarse particles in ball mill grinding," *Physicochem. Probl. Miner. Process*, vol. 52, no. 1, pp. 268–278, 2016.

[28] E. Petrakis, E. Stamboliadis, and K. Komnitsas, "Identification of optimal mill operating parameters during grinding of quartz with the use of population balance modeling," *KONA Powder Part. J.*, vol. 2017, no. 34, pp. 213–223, 2017.

[29] L. G. Austin and V. K. Bhatia, "Experimental methods for grinding studies in laboratory mills," *Powder Technol.*, vol. 5, no. 5, pp. 261–266, Apr. 1972.

[30] L. G. Austin and P. T. Luckie, "Methods for determination of breakage distribution parameters," *Powder Technol.*, vol. 5, no. 4, pp. 215–222, 1972.

[31] E. Petrakis and K. Komnitsas, "Improved Modeling of the Grinding Process through the Combined Use of Matrix and Population Balance Models," *Minerals*, vol. 7, no. 5, p. 67, 2017.

[32] D. K. Wairimu, "Characterisation of copper minerals in the Kanzugo area of the Mozambique mobile belt," University of Nairobi, 2012.

[33] A. D. Salman, M. Ghadiri, and M. J. (Michael J. . Hounslow, *Particle breakage*, Volume 12. Elsevier, 2007.

[34] S. Haner, "The Effects of Mill Conditions on Breakage Parameters of Quartz Sand in the District of Şile on the Black Sea Coast of İstanbul," in *Sand in Construction*, IntechOpen, 2022.

[35] E. G. Kelly and D. J. Spottiswood, "The breakage function; What is it really?," *Miner. Eng.*, vol. 3, no. 5, pp. 405–414, 1990.

[36] P. Semsari Parapari, M. Parian, and J. Rosenkranz, "Breakage process of mineral processing comminution machines – An approach to liberation," *Adv. Powder Technol.*, vol. 31, no. 9, pp. 3669–3685, 2020.

[37] F. M. Katubilwa and M. H. Moys, "Effect of ball size distribution on milling rate," *Miner. Eng.*, vol. 22, no. 15, pp. 1283–1288, 2009.